Am J Cancer Res 2026;16(8):3694-3709
www.ajcr.us /ISSN:2156-6976/ajcr0173699

Original Article

Incremental value of prostate-specific antigen density beyond PI-RADS and conventional MRI features for predicting the highest ISUP grade group in patients with prostate cancer diagnosed at initial systematic prostate biopsy

Dejun Fan[1*], Ruirui Niu[1*], Feiyue Zhou[1], Li Yang[1], Chunmei Zhang[2]

[1]College of Clinical Medicine, Dali University, Dali 671000, Yunnan, China; [2]Department of Pathology, The First Affiliated Hospital of Dali University, Dali 671000, Yunnan, China. [*]Equal contributors.

Received April 29, 2026; Accepted July 27, 2026; Epub August 15, 2026; Published August 30, 2026

Abstract: Objective: To evaluate the incremental value of prostate-specific antigen density (PSAD) beyond the Prostate Imaging Reporting and Data System (PI-RADS) score and conventional magnetic resonance imaging (MRI) features for predicting the highest International Society of Urological Pathology (ISUP) grade group at initial systematic biopsy. Methods: This retrospective study included 171 patients with prostate cancer diagnosed by initial systematic biopsy between February 2022 and February 2026. All patients underwent 3.0-T multiparametric MRI within 15 days before biopsy. The highest ISUP grade group across all biopsy cores was the primary outcome. A baseline model, an MRI-extended model, and a combined model incorporating PSAD were sequentially developed using proportional odds ordinal logistic regression. Internal validation was performed with 2,000 bootstrap resamples. Firth logistic regression and sensitivity analyses were used to assess robustness. Results: The numbers of patients with ISUP grade groups 1-5 were 26, 10, 9, 40, and 86, respectively; 135 patients (78.9%) had grade group ≥3. Median PSAD increased from 0.20 ng/mL^2 in grade group 1 to 1.38 ng/mL^2 in grade group 5 (P<0.001). After adjustment for age, PI-RADS score, MRI-suspected local progression, and multizonal involvement on MRI, each doubling of PSAD was associated with higher ISUP grade group (odds ratio [OR], 2.04; 95% confidence interval [CI], 1.59-2.62; P<0.001). Adding PSAD significantly improved model fit (likelihood ratio χ^2=37.83; P<0.001) and increased the bootstrap-corrected ordinal C-statistic from 0.660 to 0.744. Paired out-of-bag analysis showed a median increase of 0.094 in the ordinal C-statistic (95% CI, 0.012-0.171). The combined model achieved an out-of-bag area under the receiver operating characteristic curve of 0.835 for grade group ≥3. The association remained robust after excluding patients with total prostate-specific antigen >100 ng/mL (OR, 2.36; 95% CI, 1.68-3.29) and among patients with PI-RADS scores ≤3 (OR, 2.60; 95% CI, 1.46-5.58; P<0.001). Conclusions: PSAD was independently associated with the highest biopsy ISUP grade group and provided incremental predictive information beyond PI-RADS and conventional MRI features. PSAD may also aid in identifying patients with low PI-RADS scores but high pathological grade groups, although external validation is required.

Keywords: Prostate cancer, prostate-specific antigen density, prostate imaging reporting and data system, ISUP grade group, magnetic resonance imaging, systematic prostate biopsy

Introduction

Prostate cancer is characterized by substantial biological heterogeneity, with marked differences in progression risk, treatment strategies, and prognosis across pathological grades. The International Society of Urological Pathology (ISUP) grade group is therefore a key indicator of tumor aggressiveness and an important basis for risk stratification and clinical decision-making [1, 2]. Among patients with prostate cancer diagnosed at initial systematic prostate biopsy, pre-biopsy clinical and imaging information may facilitate a more comprehensive assessment of pathological risk.

Multiparametric magnetic resonance imaging (mpMRI) and the Prostate Imaging Reporting

https://doi.org/10.62347/BHOD8380

and Data System (PI-RADS) are widely used for prostate cancer detection and risk assessment. The PI-RADS score primarily reflects the likelihood that a lesion harbors clinically significant prostate cancer [3]. MRI findings such as extraprostatic extension and seminal vesicle invasion may also provide imaging evidence for local staging [4]. However, MRI assessments do not always correspond with biopsy findings. Discordant scenarios may occur, including positive MRI findings with negative biopsy results, as well as prostate cancer detected at biopsy despite negative or low-suspicion MRI findings [5]. Consequently, reliance on PI-RADS scores and conventional MRI features alone may result in either underestimation or overestimation of pathological risk.

Prostate-specific antigen density (PSAD), calculated as the ratio of serum total prostate-specific antigen to prostate volume, partially accounts for the influence of prostate size on PSA levels. Systematic reviews and meta-analyses have shown that PSAD can further stratify the risk of clinically significant prostate cancer beyond prostate MRI, particularly in patients with negative MRI findings or PI-RADS 3 lesions [6]. PSAD and PI-RADS provide complementary risk information, and their combined use may improve the assessment of clinically significant prostate cancer [7]. However, most previous studies in patients with PI-RADS 3 lesions or positive MRI findings have employed the presence of clinically significant prostate cancer as a binary endpoint. The incremental value of PSAD beyond PI-RADS scores and conventional MRI features for predicting the full ordinal spectrum of ISUP grade groups 1-5, as well as its potential role in identifying high-grade tumors underestimated by MRI, remains incompletely characterized [8, 9].

Accordingly, this retrospective study included patients with prostate cancer diagnosed at initial systematic prostate biopsy and used the highest ISUP grade group identified across all biopsy cores as an ordinal outcome. Hierarchical models incorporating age, PI-RADS score, conventional MRI features, and PSAD were sequentially constructed to evaluate the incremental value of PSAD in terms of model fit, discrimination, and probabilistic predictive performance. MRI-pathology phenotypes, subgroup analysis of patients with PI-RADS scores ≤3, and sensitivity analyses were further used to investigate the potential value of PSAD for additional risk stratification in patients with discordant MRI and pathological risk profiles and to assess the robustness of the findings.

Materials and methods

Study design and participants

This single-center retrospective study included 171 patients who underwent initial systematic prostate biopsy at the First Affiliated Hospital of Dali University between February 2022 and February 2026, were histopathologically diagnosed with prostate cancer, and had complete clinical, imaging, and pathological data.

The inclusion criteria were as follows: (1) Undergoing systematic prostate biopsy for the first time; (2) Completion of 3.0-T multiparametric MRI within 15 days before biopsy, and interpreted according to PI-RADS version 2.1; and (3) Complete data on total prostate-specific antigen (tPSA), three-dimensional prostate measurements, PI-RADS score, and biopsy pathology, including a clearly documented Gleason score and ISUP grade group. The exclusion criteria were as follows: (1) A history of previous prostate biopsy; (2) Receipt of prostate cancer-related treatment before biopsy; (3) Receipt of MRI-targeted biopsy or combined systematic and MRI-targeted biopsy; and (4) Incomplete key clinical, imaging, or pathological data.

The study was approved by the Ethics Committee of the First Affiliated Hospital of Dali University, which waived the requirement for informed consent. The ethics approval number was DFY20260205001.

MRI examination, prostate biopsy, and pathological assessment

All patients underwent multiparametric MRI using a 3.0-T MRI system (Toshiba Medical Systems, Japan) within 15 days before biopsy. MRI examinations were independently interpreted by two radiologists, each with more than 10 years of experience in prostate MRI. Disagreements were adjudicated by consensus. The patient-level PI-RADS score was defined as the highest score among all identified lesions and was categorized as PI-RADS ≤3,

PI-RADS 4, or PI-RADS 5 in the primary analysis. MRI evidence of extraprostatic extension or seminal vesicle invasion was defined as MRI-suspected local progression. The anatomical zones involved by the lesions were recorded on MRI, and involvement of at least two anatomical zones was defined as MRI multizonal involvement.

All patients underwent initial systematic prostate biopsy without MRI-targeted biopsy. Biopsies were performed through either the transrectal or transperineal approach. The total number of biopsy cores, number of positive cores, and pathological findings were recorded. Biopsy specimens were routinely fixed, paraffin-embedded, and stained with hematoxylin and eosin. The specimens were evaluated by pathologists at our institution with experience in prostate pathology, and the pathological findings were reported according to the Gleason scoring system and ISUP grade group criteria. Difficult cases were reviewed in accordance with routine departmental practice. The highest Gleason score and corresponding ISUP grade group identified across all biopsy cores were recorded for each patient. The proportion of tumor tissue in the biopsy core corresponding to the highest ISUP grade group was recorded for descriptive purposes only, not as a predictor.

Clinical variables, prostate volume, and PSAD calculation

Data on age, body mass index (BMI), serum total prostate-specific antigen (tPSA), and the anteroposterior, transverse, and craniocaudal diameters of the prostate were collected. All three prostate diameters were measured in centimeters. Prostate volume was calculated using the ellipsoid formula:

Prostate volume (mL) = 0.52 × anteroposterior diameter × transverse diameter × craniocaudal diameter.

Prostate-specific antigen density (PSAD) was calculated as the ratio of tPSA to prostate volume. For 53 patients, tPSA was recorded in the hospital information system only as “>100 ng/mL”, and the exact values were unavailable. Therefore, a value of 100 ng/mL was uniformly imputed for PSAD calculation, without extrapolation beyond this threshold. All subsequent references to PSAD indicate values calculated according to this rule.

For regression analyses, PSAD was log-transformed to base 2 [$\log_2$(PSAD)] and entered into the models as a continuous variable. The reported odds ratios therefore represent the relative change in the odds of being classified into a higher outcome category for each doubling of PSAD. Descriptive statistics and graphical presentations used the original PSAD values and units, with logarithmic scales applied to the PSAD axes where appropriate.

Study outcomes and MRI-pathology phenotypes

The primary outcome was the highest ISUP grade group identified across all biopsy cores, analyzed as an ordinal outcome with five categories ranging from grade group 1 to 5. The secondary outcome was an ISUP grade group of ≥3.

To describe concordance between the PI-RADS category and the highest biopsy ISUP grade group, patients were classified into four prespecified MRI-pathology phenotypes. Patients with PI-RADS ≤3 and ISUP grade group ≤2 were classified as concordant low, those with PI-RADS ≤3 and ISUP grade group ≥3 as MRI-underestimated, those with PI-RADS ≥4 and ISUP grade group ≤2 as MRI-overestimated, and those with PI-RADS ≥4 and ISUP grade group ≥3 as concordant high. The association between PSAD and ISUP grade group ≥3 was further examined among patients with PI-RADS ≤3 to evaluate the complementary value of PSAD for risk stratification in patients with relatively low PI-RADS scores.

These operational categories were based on prespecified thresholds for the PI-RADS category and highest biopsy ISUP grade group, and served solely to describe concordance between MRI assessment and biopsy pathology and do not represent a formal clinical risk-stratification system.

Model development and internal validation

The primary analysis was performed using proportional-odds ordinal logistic regression. The models were estimated across four cumulative thresholds - ISUP grade group ≤1 versus >1, ≤2

versus >2, ≤3 versus >3, and ≤4 versus >4 - under the assumption that the regression coefficient for each predictor was constant across these thresholds. Model effects were expressed as common odds ratios (ORs) with 95% confidence intervals (CIs), with an OR >1 indicating increased odds of being classified into a higher ISUP grade group.

Three hierarchical models were prespecified. Model 1 included age and PI-RADS category. Model 2 added MRI-suspected local progression and MRI multizonal involvement to Model 1. Model 3 further incorporated PSAD into Model 2. Age was modeled per 10-year increase, and PI-RADS ≤3 was used as the reference category. All predictors were prespecified on the basis of clinical relevance; no univariable screening, stepwise regression, least absolute shrinkage and selection operator selection, or data-driven cutoff selection was performed.

Adjacent hierarchical models were compared using likelihood ratio tests, and the Akaike information criterion (AIC), Bayesian information criterion (BIC), and Nagelkerke R^2 were reported. The proportional-odds assumption was assessed using a Brant test, and multicollinearity among predictors was evaluated using variance inflation factors. The incremental contribution of each predictor was assessed by sequentially removing individual predictors from the full model and comparing the resulting nested models using partial likelihood ratio χ^2 statistics.

A linear effect of $\log_2$-transformed PSAD, corresponding to a doubling of PSAD, was prespecified as the primary functional form. The association between PSAD and the highest ISUP grade group was further examined using a four-knot restricted cubic spline based on $\log_2$ (PSAD), with knots placed at the 5th, 35th, 65th, and 95th percentiles of its distribution. The restricted cubic spline model was compared with the prespecified linear model using a likelihood ratio test to assess the joint contribution of the two nonlinear spline terms.

Internal validation was performed using 2,000 patient-level bootstrap resamples. Apparent and optimism-corrected performance was estimated for the ordinal C-statistic, ranked probability score (RPS), log loss, and Nagelkerke R^2. Bootstrap samples that did not contain all five ISUP grade groups were discarded and redrawn.

For each patient, predicted probabilities obtained from bootstrap resamples in which that patient was not selected were averaged to generate mean out-of-bag predicted probabilities. These predictions were used to evaluate the area under the receiver operating characteristic curve (AUROC), average precision (AP), Brier score, calibration intercept, and calibration slope for ISUP grade group ≥2, ≥3, ≥4, and grade group 5. The 95% CIs for these performance measures were estimated using 2,000 patient-level bootstrap resamples. Calibration curves were smoothed using mildly ridge-penalized cubic splines and were used solely to illustrate the relationship between predicted probabilities and observed outcomes. Given the limited sample size, the dataset was retained as a single cohort for development, rather than randomly split into training and validation sets.

Statistical and sensitivity analyses

Continuous variables are presented as medians with interquartile ranges and were compared across ISUP grade groups using the Kruskal-Wallis test. Categorical variables are presented as counts and percentages and were compared using a Pearson χ^2 test based on 20,000 permutations. Because all included patients had complete data for the principal clinical, imaging, and pathological variables, no missing-data imputation was performed in the primary analysis.

Sensitivity analyses were conducted by: (1) Excluding patients with tPSA >100 ng/mL; (2) Modeling the original PI-RADS score as a continuous variable per 1-point increase; (3) Categorizing MRI lesion extent as no suspicious lesion, single-zone involvement, or multizonal involvement; (4) Restricting the analysis to patients who underwent transrectal biopsy; (5) Additionally adjusting for biopsy approach and total number of biopsy cores; and (6) Additionally adjusting for BMI. These analyses were performed to assess the robustness of the estimated PSAD effect across alternative model specifications and analytic populations.

Secondary analyses with ISUP grade group ≥3 as the outcome were performed using Firth

penalized logistic regression. The overall model included age, PI-RADS category, MRI-suspected local progression, MRI multizonal involvement, and PSAD, whereas the model restricted to patients with PI-RADS ≤3 included age and PSAD. Both models additionally included an indicator for whether the original tPSA record was >100 ng/mL to account for differences in tPSA recording; the effect of this indicator was not interpreted clinically.

The 95% CIs for the PSAD effect were estimated using profile penalized likelihood, and *P* values were calculated using penalized likelihood ratio tests. For the remaining covariates, 95% CIs and *P* values were obtained using Wald methods based on the Fisher information matrix. No adjustment for multiple comparisons was applied to the sensitivity analyses. All tests were two-sided, and P<0.05 was considered statistically significant. Statistical analyses were performed using Python version 3.12.13.

Results

Patient characteristics

A total of 171 patients were included. The numbers of patients with highest ISUP grade groups 1, 2, 3, 4, and 5 were 26, 10, 9, 40, and 86, respectively; 135 patients (78.9%) had ISUP grade group ≥3. The median age was 72 years (interquartile range [IQR], 68-76 years), the median tPSA level was 37.2 ng/mL (IQR, 15.6-100.0 ng/mL), the median prostate volume was 47.29 mL (IQR, 32.50-62.88 mL), and the median PSAD was 0.82 ng/mL^2 (IQR, 0.34-1.73 ng/mL^2).

PI-RADS ≤3, PI-RADS 4, and PI-RADS 5 were recorded in 48 (28.1%), 50 (29.2%), and 73 (42.7%) patients, respectively. MRI-suspected local progression was present in 70 patients (40.9%), and MRI multizonal involvement was present in 54 (31.6%). Transrectal and transperineal biopsy were performed in 143 (83.6%) and 28 (16.4%) patients, respectively.

Median PSAD rose from 0.20 ng/mL^2 in ISUP grade group 1 to 1.38 ng/mL^2 in grade group 5, with a significant difference across grade groups (P<0.001). PI-RADS category, MRI-suspected local progression and its component findings, MRI lesion extent, number of positive biopsy cores, and the proportion of tumor tissue in the core corresponding to the highest ISUP grade group also differed across ISUP grade groups (**Table 1**).

Model diagnostics and primary ordinal regression results

For Model 3, the global test of the proportional-odds assumption yielded χ^2=25.27 with 18 degrees of freedom (P=0.118), providing no clear evidence of an overall violation of the assumption. In predictor-specific tests, MRI multizonal involvement reached statistical significance (χ^2=8.28, df=3, P=0.041), suggesting some degree of heterogeneity in its effect across cumulative thresholds. No evidence of a violation was observed for PSAD (χ^2=1.59, df=3, P=0.662), and the direction of its association was consistent across all cumulative thresholds. Variance inflation factors ranged from 1.07 to 2.26, indicating no substantial multicollinearity. Restricted cubic spline analysis provided no clear evidence of a nonlinear association between PSAD and the highest ISUP grade group (likelihood ratio [LR] χ^2= 5.32, df=2, P=0.070); therefore, the prespecified linear effect per doubling of PSAD was retained in the primary analysis.

Comparison of the hierarchical models showed that adding MRI-suspected local progression and MRI multizonal involvement significantly improved model fit in Model 2 compared with Model 1 (LR χ^2=10.98, df=2, P=0.004). The AIC decreased from 439.1 to 432.1, the BIC decreased from 461.1 to 460.4, and the apparent Nagelkerke R^2 increased from 0.103 to 0.163. The subsequent addition of PSAD further improved model fit in Model 3 compared with Model 2 (LR χ^2=37.83, df=1, P< 0.001). The AIC decreased from 432.1 to 396.3, the BIC decreased from 460.4 to 427.7, and the apparent Nagelkerke R^2 increased from 0.163 to 0.346, indicating substantial improvement in model fit and explained variation after PSAD was incorporated.

In Model 3, each doubling of PSAD was associated with a 2.04-fold increase in the odds of being classified into a higher ISUP grade group (OR, 2.04; 95% CI, 1.59-2.62; P<0.001). PSAD remained independently associated with the highest ISUP grade group after simultaneous adjustment for age, PI-RADS category, MRI-

Table 1. Patient characteristics stratified by the highest ISUP grade group

Characteristic	Overall (n=171)	ISUP grade group 1 (n=26)	ISUP grade group 2 (n=10)	ISUP grade group 3 (n=9)	ISUP grade group 4 (n=40)	ISUP grade group 5 (n=86)	*P* value
Age, years	72.00 (68.00-76.00)	71.00 (62.25-73.75)	73.00 (70.50-79.00)	74.00 (71.00-76.00)	71.00 (68.75-76.00)	73.00 (68.00-77.00)	0.307
BMI, kg/m^2	22.04 (20.20-24.32)	21.50 (19.85-24.02)	22.33 (19.45-24.35)	21.63 (21.05-23.67)	21.57 (20.15-24.43)	22.17 (20.20-24.65)	0.969
tPSA, ng/mL	37.2 (15.6-100.0)	10.29 (7.36-21.79)	11.71 (7.74-27.41)	19.97 (13.04-37.25)	30.4 (15.3-100.0)	81.7 (35.0-100.0)	<0.001
Prostate volume, mL	47.29 (32.50-62.88)	55.35 (43.11-85.58)	37.03 (28.78-41.65)	51.17 (28.39-59.67)	47.26 (32.39-58.06)	48.28 (32.23-61.22)	0.211
PSAD, ng/mL^2	0.82 (0.34-1.73)	0.20 (0.13-0.40)	0.30 (0.21-0.89)	0.62 (0.33-0.76)	0.63 (0.33-1.79)	1.38 (0.72-1.93)	<0.001
Tumor involvement in the biopsy core with the highest ISUP grade group, %	60.00 (20.00-80.00)	20.00 (6.25-30.00)	55.00 (15.00-60.00)	50.00 (30.00-80.00)	70.00 (27.50-80.00)	70.00 (40.00-80.00)	<0.001
Positive biopsy cores, n	8.00 (4.00-12.00)	2.00 (1.00-3.00)	5.50 (3.25-10.50)	6.00 (2.00-7.00)	6.50 (4.00-9.00)	11.00 (8.00-12.00)	<0.001
Total biopsy cores, n	13.00 (12.00-15.00)	13.00 (12.00-15.50)	13.00 (12.00-14.00)	13.00 (12.00-19.00)	13.00 (12.00-15.25)	13.00 (12.00-14.00)	0.847
PI-RADS category							0.002
≤3	48 (28.1)	15 (57.7)	4 (40.0)	4 (44.4)	8 (20.0)	17 (19.8)	
4	50 (29.2)	9 (34.6)	3 (30.0)	1 (11.1)	13 (32.5)	24 (27.9)	
5	73 (42.7)	2 (7.7)	3 (30.0)	4 (44.4)	19 (47.5)	45 (52.3)	
MRI-suspected local progression	70 (40.9)	2 (7.7)	1 (10.0)	1 (11.1)	19 (47.5)	47 (54.7)	<0.001
MRI-suspected extraprostatic extension	65 (38.0)	2 (7.7)	1 (10.0)	1 (11.1)	15 (37.5)	46 (53.5)	<0.001
MRI-suspected seminal vesicle invasion	36 (21.1)	0 (0.0)	0 (0.0)	0 (0.0)	12 (30.0)	24 (27.9)	0.003
MRI lesion extent							0.003
No suspicious lesion	12 (7.0)	6 (23.1)	1 (10.0)	0 (0.0)	4 (10.0)	1 (1.2)	
Single-zone involvement	105 (61.4)	17 (65.4)	6 (60.0)	9 (100.0)	22 (55.0)	51 (59.3)	
Multizonal involvement	54 (31.6)	3 (11.5)	3 (30.0)	0 (0.0)	14 (35.0)	34 (39.5)	
Biopsy approach							0.068
Transrectal	143 (83.6)	22 (84.6)	10 (100.0)	5 (55.6)	36 (90.0)	70 (81.4)	
Transperineal	28 (16.4)	4 (15.4)	0 (0.0)	4 (44.4)	4 (10.0)	16 (18.6)	

Note: Continuous variables are presented as median (first quartile-third quartile), and categorical variables as number (column percentage). Continuous variables were compared across groups using the Kruskal-Wallis test, and categorical variables were compared using a permutation test based on the Pearson χ^2 statistic with 20,000 permutations. All tests were two-sided. For patients whose tPSA was recorded in the hospital information system as ">100 ng/mL", a value of 100 ng/mL was used for both descriptive analyses and PSAD calculation. BMI, body mass index; tPSA, total prostate-specific antigen; PSAD, prostate-specific antigen density; PI-RADS, Prostate Imaging Reporting and Data System; MRI, magnetic resonance imaging; ISUP, International Society of Urological Pathology.

Table 2. Effect estimates and fit indices for the three hierarchical proportional-odds ordinal logistic regression models

Item	Model 1	Model 2	Model 3
Regression effects, OR (95% CI); *P* value			
Age, per 10-year increase	1.19 (0.80-1.77); P=0.387	1.21 (0.81-1.80); P=0.362	1.04 (0.68-1.58); P=0.869
PI-RADS 4 vs ≤3	2.05 (0.97-4.34); P=0.062	1.54 (0.71-3.34); P=0.280	1.19 (0.53-2.67); P=0.671
PI-RADS 5 vs ≤3	3.93 (1.91-8.11); P<0.001	1.84 (0.79-4.28); P=0.156	1.77 (0.74-4.23); P=0.202
MRI-suspected local progression	-	2.92 (1.44-5.93); P=0.003	1.33 (0.61-2.93); P=0.476
MRI multizonal involvement	-	1.44 (0.71-2.90); P=0.308	1.17 (0.56-2.41); P=0.679
PSAD, per doubling	-	-	2.04 (1.59-2.62); P<0.001
Model fit and hierarchical comparisons			
Log likelihood	-212.563	-207.072	-188.157
AIC	439.1	432.1	396.3
BIC	461.1	460.4	427.7
Apparent Nagelkerke R^2	0.103	0.163	0.346
Likelihood ratio test vs preceding model	-	χ^2=10.98; df=2; P=0.004	χ^2=37.83; df=1; P<0.001

Note: Regression effects are presented as common ORs with 95% CIs and *P* values. An OR >1 indicates increased odds of being classified into a higher ISUP grade group. Model 1 included age and PI-RADS category. Model 2 additionally included MRI-suspected local progression and MRI multizonal involvement. Model 3 further incorporated PSAD. The OR for PSAD is interpreted per doubling of PSAD. Lower AIC and BIC values indicate relatively better model performance after accounting for both goodness of fit and model complexity. AIC, Akaike information criterion; BIC, Bayesian information criterion; CI, confidence interval; df, degrees of freedom; ISUP, International Society of Urological Pathology; MRI, magnetic resonance imaging; OR, odds ratio; PI-RADS, Prostate Imaging Reporting and Data System; PSAD, prostate-specific antigen density.

suspected local progression, and MRI multizonal involvement. None of the remaining predictors reached statistical significance (**Table 2** and **Figure 1**).

Internal validation and predictive performance

The apparent/optimism-corrected ordinal C-statistics for Models 1, 2, and 3 were 0.637/0.622, 0.685/0.660, and 0.763/0.744, respectively. The corresponding RPS values were 0.674/0.701, 0.644/0.680, and 0.529/0.565; log-loss values were 1.243/1.285, 1.211/1.266, and 1.100/1.163; and Nagelkerke R^2 values were 0.103/0.066, 0.163/0.105, and 0.346/0.287. In the paired out-of-bag analysis, the median increase in the ordinal C-statistic for Model 3 versus Model 2 was 0.094 (95% CI, 0.012-0.171), whereas the median difference in RPS (Model 3 minus Model 2) was -0.119 (95% CI, -0.200 to 0.002). These findings indicate that the addition of PSAD improved overall discrimination and generally reduced the RPS, although the 95% CI for the RPS difference included zero (**Table 3** and **Figure 2**).

The out-of-bag AUROCs of Model 3 for predicting ISUP grade group ≥2, ≥3, ≥4, and grade group 5 were 0.866, 0.835, 0.830, and 0.739, respectively. The corresponding AP values were 0.974, 0.948, 0.934, and 0.641, and the calibration slopes were 1.26, 1.10, 1.07, and 0.75, respectively. Calibration slopes were generally close to 1 for the first three cumulative outcomes, whereas the lower slope for grade group 5 suggested that the predicted probabilities for the highest-grade outcome may have been overly extreme (**Table 4** and **Figure 3**).

MRI-pathology phenotypes and sensitivity analyses

Based on the prespecified combinations of PI-RADS category and highest biopsy ISUP grade group, 19, 29, 17, and 106 patients were classified as concordant low, MRI-underestimated, MRI-overestimated, and concordant high, respectively. Among the 48 patients with PI-RADS ≤3, 29 (60.4%) had ISUP grade group ≥3. Median PSAD was numerically higher in the MRI-underestimated group than in the concordant-low group (0.71 ng/mL^2 [IQR, 0.34-1.72] vs 0.20 ng/mL^2 [IQR, 0.11-0.40]) (**Figure 4A** and **4B**).

After excluding the 53 patients with tPSA >100 ng/mL, 118 patients remained, of whom 83 had ISUP grade group ≥3. In the proportional-odds ordinal logistic regression analysis, the OR per doubling of PSAD was 2.36 (95% CI,

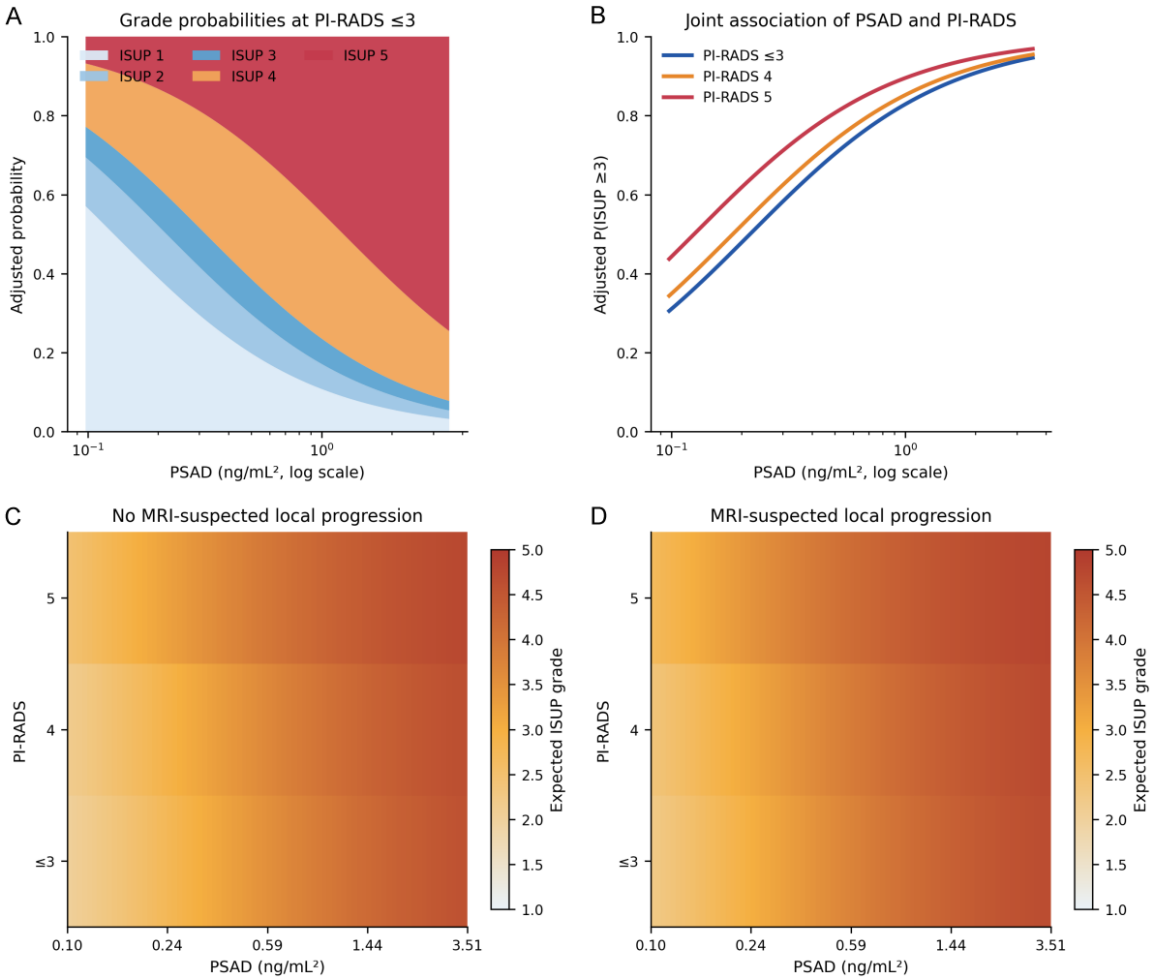

Figure 1. Adjusted associations of PSAD with the highest biopsy ISUP grade group in Model 3. A. Adjusted predicted probabilities of ISUP grade groups 1-5 across PSAD levels among patients with PI-RADS ≤3; B. Adjusted predicted probability of ISUP grade group ≥3 across PSAD levels according to PI-RADS category; C and D. Associations of PSAD and PI-RADS category with the expected ISUP grade group in the absence and presence of MRI-suspected local progression, respectively. Age was fixed at the overall median, and MRI multizonal involvement was set as absent. PSAD was displayed from the 5th to the 95th percentile. The results shown are adjusted predictions derived from the final fitted model. PSAD, prostate-specific antigen density; PI-RADS, Prostate Imaging Reporting and Data System; MRI, magnetic resonance imaging; ISUP, International Society of Urological Pathology.

Table 3. Bootstrap internal validation performance of the three ordinal logistic regression models

Performance metric	Model 1	Model 2	Model 3
Ordinal C-statistic (apparent/optimism-corrected)	0.637/0.622	0.685/0.660	0.763/0.744
RPS (apparent/optimism-corrected)	0.674/0.701	0.644/0.680	0.529/0.565
Log loss (apparent/optimism-corrected)	1.243/1.285	1.211/1.266	1.100/1.163
Nagelkerke R^2 (apparent/optimism-corrected)	0.103/0.066	0.163/0.105	0.346/0.287

Note: Values are presented as apparent performance/bootstrap optimism-corrected performance. Internal validation was performed using 2,000 patient-level bootstrap resamples. Model 1 included age and PI-RADS category. Model 2 additionally included MRI-suspected local progression and MRI multizonal involvement. Model 3 further incorporated PSAD. Higher ordinal C-statistic and Nagelkerke R^2 values indicate better model performance, whereas lower RPS and log-loss values indicate smaller prediction errors. MRI, magnetic resonance imaging; PI-RADS, Prostate Imaging Reporting and Data System; PSAD, prostate-specific antigen density; RPS, ranked probability score.

1.68-3.29; P<0.001). The effect estimate for PSAD remained stable when PI-RADS was modeled as a continuous variable, MRI lesion extent was alternatively categorized, the analy-

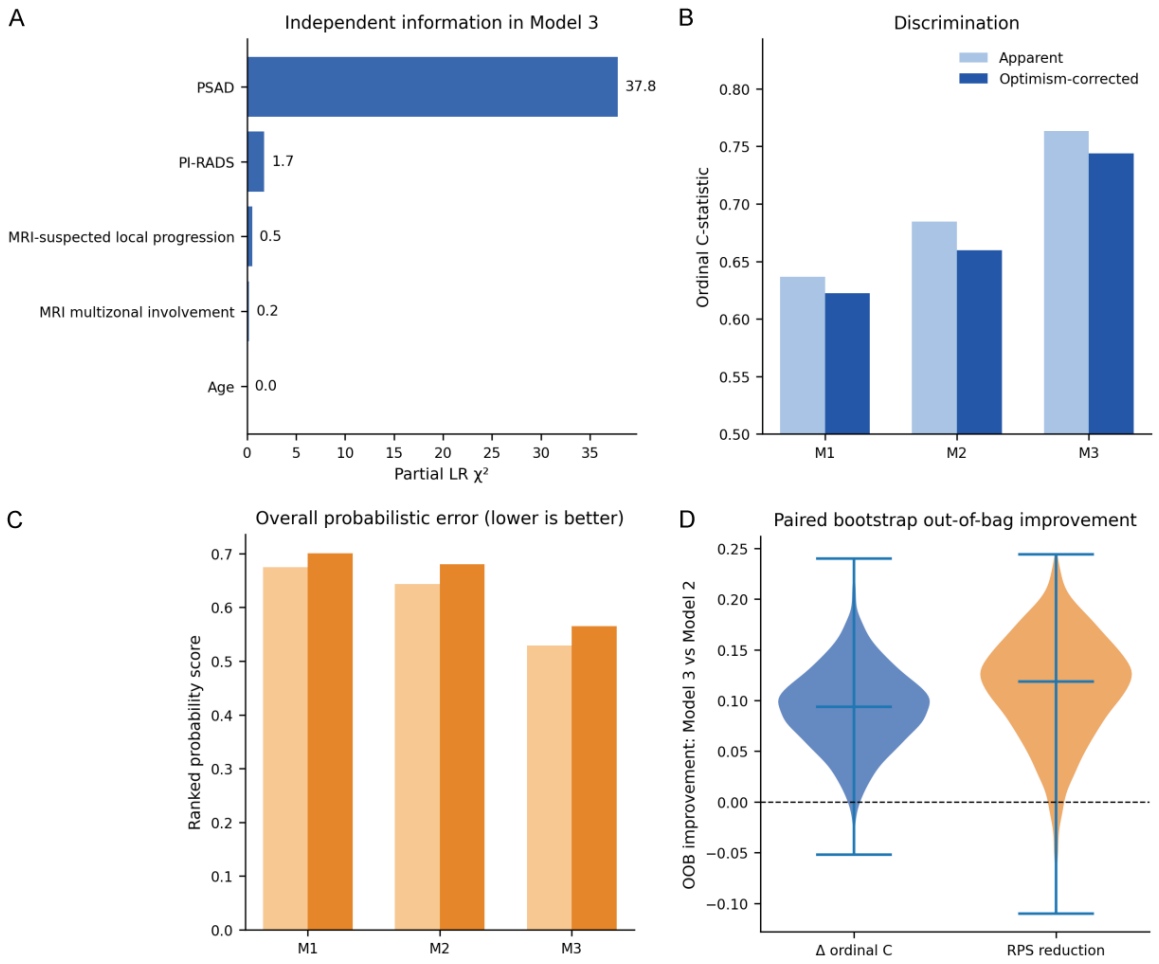

Figure 2. Incremental information from the hierarchical models and results of bootstrap internal validation. (A) Partial likelihood ratio χ^2 statistics for each predictor group in Model 3; (B) Apparent and bootstrap-corrected ordinal C-statistics for Models 1-3; (C) Apparent and bootstrap-corrected ranked probability scores for Models 1-3; and (D) Differences in performance between Model 3 and Model 2 across 2,000 paired out-of-bag bootstrap resamples. The horizontal line indicates the median, the vertical capped line indicates the minimum-to-maximum range of the paired out-of-bag bootstrap distribution, and the horizontal dashed line indicates no difference in performance between the two models. M1-M3, Models 1-3; RPS, ranked probability score; OOB, out-of-bag; CI, confidence interval.

Table 4. Cumulative-threshold discrimination and calibration performance of Model 3 based on mean out-of-bag predictions

Threshold	Events, n/N (%)	AUROC (95% CI)	Average precision (95% CI)	Brier score (95% CI)	Calibration intercept (95% CI)	Calibration slope (95% CI)
ISUP grade group ≥2	145/171 (84.8)	0.866 (0.794-0.922)	0.974 (0.955-0.988)	0.097 (0.071-0.126)	-0.28 (-1.10-0.41)	1.26 (0.89-1.84)
ISUP grade group ≥3	135/171 (78.9)	0.835 (0.764-0.900)	0.948 (0.916-0.975)	0.123 (0.094-0.153)	-0.04 (-0.65-0.54)	1.10 (0.78-1.60)
ISUP grade group ≥4	126/171 (73.7)	0.830 (0.763-0.889)	0.934 (0.896-0.964)	0.143 (0.114-0.174)	0.01 (-0.51-0.48)	1.07 (0.78-1.49)
ISUP grade group 5	86/171 (50.3)	0.739 (0.660-0.812)	0.641 (0.547-0.756)	0.205 (0.173-0.240)	0.06 (-0.27-0.41)	0.75 (0.49-1.09)

Note: The predictive performance of Model 3 was calculated using each patient's mean out-of-bag predicted probabilities obtained from 2,000 bootstrap resamples. Values in parentheses are 95% CIs estimated using 2,000 patient-level bootstrap resamples. The no-information baseline for average precision was the event prevalence at the corresponding outcome threshold. Higher AUROC and average precision values and lower Brier scores indicate better predictive performance. The ideal calibration intercept is 0, and the ideal calibration slope is 1. AUROC, area under the receiver operating characteristic curve; CI, confidence interval; ISUP, International Society of Urological Pathology.

sis was restricted to patients undergoing transrectal biopsy, or further adjustment was made for biopsy approach, total number of biopsy cores, or BMI; the corresponding ORs ranged

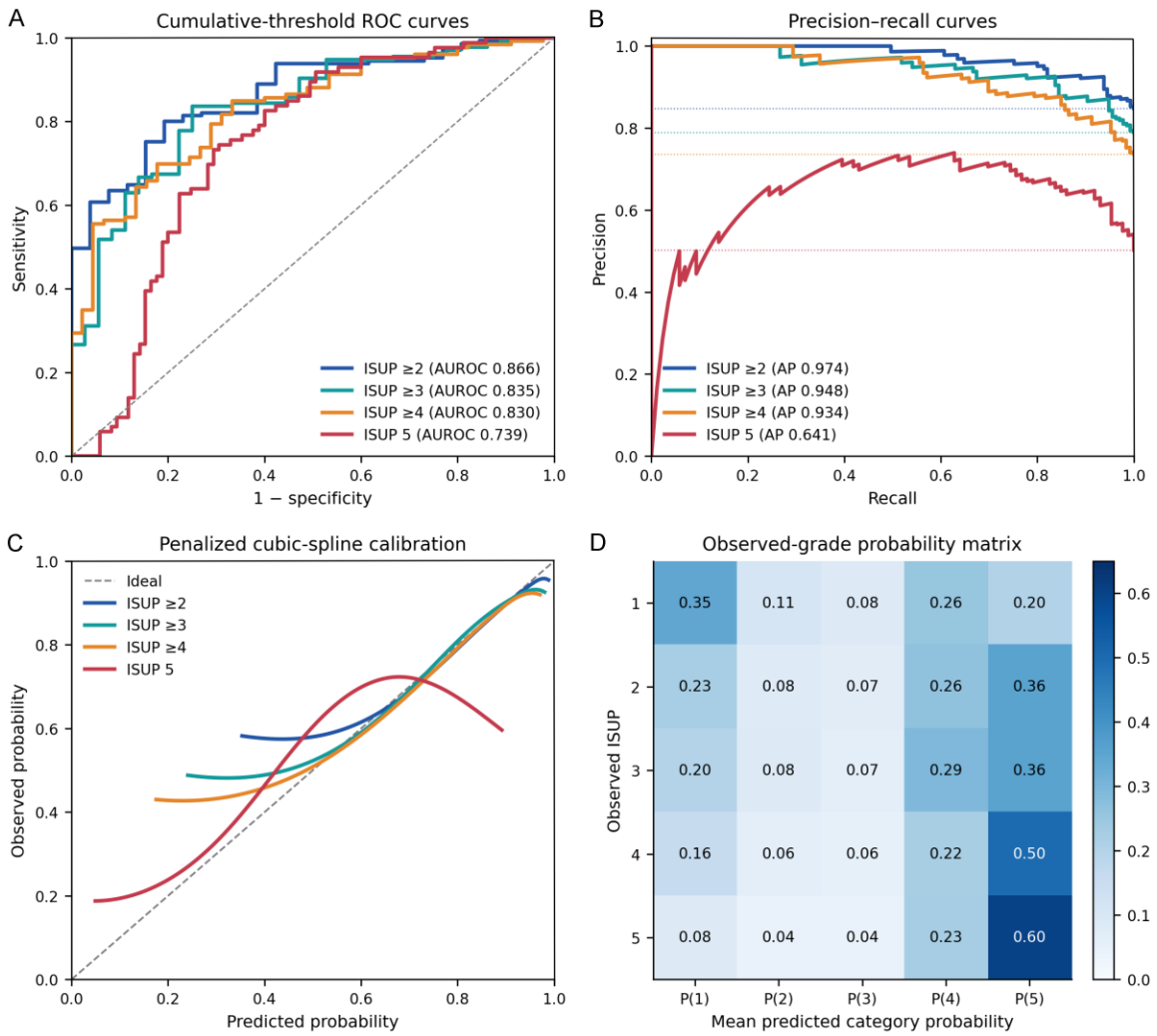

Figure 3. Internally validated performance of Model 3 based on mean bootstrap out-of-bag predicted probabilities. (A) Receiver operating characteristic curves for ISUP grade group ≥2, ≥3, ≥4, and grade group 5; (B) Corresponding precision-recall curves, with horizontal dash-dotted lines indicating the event prevalence; (C) Calibration curves, with the gray dashed line indicating ideal calibration; and (D) Matrix of mean predicted class probabilities for each observed ISUP grade group. Patient-level predicted probabilities were calculated as mean out-of-bag predictions obtained from 2,000 bootstrap resamples. ROC, receiver operating characteristic; AUROC, area under the receiver operating characteristic curve; PR, precision-recall; AP, average precision; ISUP, International Society of Urological Pathology.

from 2.02 to 2.21, with all *P* values <0.001 (**Table 5** and **Figure 4D**). In the multivariable Firth logistic regression analysis for ISUP grade group ≥3, each doubling of PSAD remained independently associated with the outcome after adjustment for age, PI-RADS category, MRI-suspected local progression, MRI multizonal involvement, and the indicator for tPSA recording status (OR, 1.99; profile penalized-likelihood 95% CI, 1.39-3.03; P<0.001), whereas the remaining clinically evaluated covariates were not statistically significant (all P>0.05; **Table 6**).

In the Firth logistic regression analysis restricted to patients with PI-RADS ≤3, each doubling of PSAD remained significantly associated with ISUP grade group ≥3 after adjustment for age and the tPSA recording-status indicator (OR, 2.60; profile penalized-likelihood 95% CI, 1.46-5.58; P<0.001). This finding suggests that PSAD may provide complementary information for identifying pathological risk among patients with relatively low PI-RADS scores (**Table 5** and **Figure 4C**, **4D**). The direction of the PSAD association was consistent across the primary ordinal analysis, secondary

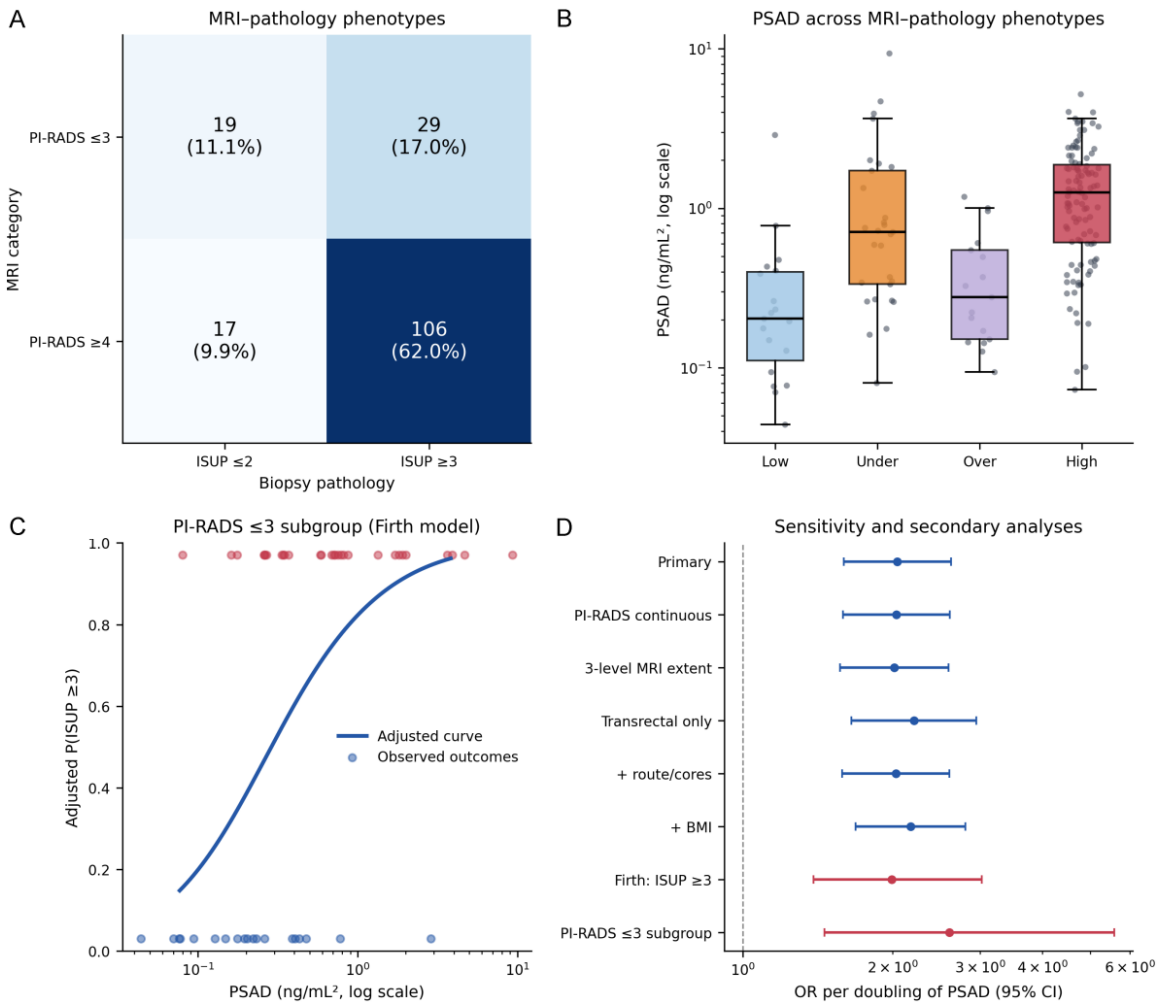

Figure 4. MRI-pathology phenotypes and robustness analyses of the PSAD effect. (A) Four MRI-pathology phenotypes defined according to PI-RADS category and the highest biopsy ISUP grade group; (B) Distribution of PSAD across the phenotypes, with the y-axis displayed on a logarithmic scale; (C) Association between PSAD and the adjusted predicted probability of ISUP grade group ≥3 in the PI-RADS ≤3 subgroup; and (D) Odds ratios with 95% confidence intervals per doubling of PSAD in the primary analysis, sensitivity analyses, and Firth logistic regression analyses. The vertical dashed line indicates an odds ratio of 1. The result obtained after excluding patients with tPSA >100 ng/mL is presented in **Table 5**. OR, odds ratio; CI, confidence interval; PSAD, prostate-specific antigen density; tPSA, total prostate-specific antigen; PI-RADS, Prostate Imaging Reporting and Data System; MRI, magnetic resonance imaging; ISUP, International Society of Urological Pathology.

binary analysis, sensitivity analyses, and the PI-RADS ≤3 subgroup analysis, supporting the incremental pathological risk information provided by PSAD beyond PI-RADS and conventional MRI features.

Discussion

In this study, the highest ISUP grade group identified at initial systematic prostate biopsy was analyzed as an ordinal outcome to evaluate the incremental value of PSAD beyond the PI-RADS score and conventional MRI features. After adjustment for age, PI-RADS category, MRI-suspected local progression, and MRI multizonal involvement, each doubling of PSAD was associated with a 2.04-fold increase in the odds of being classified into a higher ISUP grade group. Adding PSAD substantially improved model fit and explained variation, and increased the bootstrap optimism-corrected ordinal C-statistic from 0.660 to 0.744. In the paired out-of-bag analysis, the median increase in the ordinal C-statistic was 0.094. The RPS also generally decreased, although the 95% CI for the difference included zero. Collectively,

Table 5. Primary, secondary, and sensitivity analyses of the association between PSAD and ISUP grade group

Analysis	N	ISUP grade group ≥3, n	PSAD OR (95% CI)	*P* value	Model
Primary analysis: PSAD	171	135	2.04 (1.59-2.62)	<0.001	Ordinal logistic regression
Excluding patients with tPSA >100 ng/mL	118	83	2.36 (1.68-3.29)	<0.001	Ordinal logistic regression
PI-RADS modeled per 1-point increase	171	135	2.04 (1.59-2.61)	<0.001	Ordinal logistic regression
MRI lesion extent modeled as none/single-zone/multizonal involvement	171	135	2.02 (1.57-2.59)	<0.001	Ordinal logistic regression
Restricted to transrectal biopsy	143	111	2.21 (1.65-2.95)	<0.001	Ordinal logistic regression
Additional adjustment for biopsy approach and total number of biopsy cores	171	135	2.03 (1.58-2.60)	<0.001	Ordinal logistic regression
Additional adjustment for BMI	171	135	2.17 (1.69-2.80)	<0.001	Ordinal logistic regression
Secondary outcome: ISUP grade group ≥3	171	135	1.99 (1.39-3.03)	<0.001	Firth logistic regression
PI-RADS ≤3 subgroup: ISUP grade group ≥3	48	29	2.60 (1.46-5.58)	<0.001	Firth logistic regression

Note: All ORs for PSAD are interpreted per doubling of PSAD. The ordinal logistic regression analyses used the highest biopsy ISUP grade group, ranging from 1 to 5, as the outcome; the column "ISUP grade group ≥3, n" indicates only the number of patients meeting this threshold within each analytic sample. Unless otherwise specified, the covariate structure of the primary model was retained. Analyses with ISUP grade group ≥3 as the outcome were performed using Firth logistic regression. For PSAD in the Firth models, 95% CIs were estimated using profile penalized likelihood, and *P* values were obtained using penalized likelihood ratio tests. No adjustment for multiple comparisons was applied to the sensitivity analyses. BMI, body mass index; CI, confidence interval; ISUP, International Society of Urological Pathology; MRI, magnetic resonance imaging; OR, odds ratio; PI-RADS, Prostate Imaging Reporting and Data System; PSAD, prostate-specific antigen density; tPSA, total prostate-specific antigen.

Table 6. Multivariable Firth logistic regression analysis for ISUP grade group ≥3

Predictor	OR (95% CI)	*P* value
Age, per 10-year increase	1.21 (0.66-2.19)	0.538
PI-RADS 4 vs ≤3	1.18 (0.43-3.22)	0.751
PI-RADS 5 vs ≤3	2.95 (0.84-10.31)	0.091
MRI-suspected local progression	1.88 (0.49-7.15)	0.355
MRI multizonal involvement	0.84 (0.27-2.66)	0.771
PSAD, per doubling	1.99 (1.39-3.03)	<0.001

Note: The outcome was highest biopsy ISUP grade group ≥3. The analysis included 171 patients, of whom 135 met the outcome. The model included age, PI-RADS category, MRI-suspected local progression, MRI multizonal involvement, PSAD, and an indicator for tPSA recorded as >100 ng/mL. The latter was included solely for technical adjustment and is therefore not shown. The OR for PSAD is interpreted per doubling of PSAD. For PSAD, the 95% CI was estimated using profile penalized likelihood, and the *P* value was obtained using a penalized likelihood ratio test; Wald methods were used for the remaining predictors. CI, confidence interval; ISUP, International Society of Urological Pathology; MRI, magnetic resonance imaging; OR, odds ratio; PI-RADS, Prostate Imaging Reporting and Data System; PSAD, prostate-specific antigen density; tPSA, total prostate-specific antigen.

these findings suggest that PSAD provides additional information on pathological grade beyond PI-RADS and conventional MRI features, particularly by improving overall discrimination across ISUP grade groups.

PI-RADS stratifies the risk of clinically significant prostate cancer according to lesion characteristics across different MRI sequences. Nevertheless, substantial heterogeneity can remain within the same PI-RADS category. MRI features such as lesion volume, shape, and dimensions may provide information beyond the PI-RADS category and may further influence the detection of clinically significant prostate cancer [10, 11]. MRI findings of extraprostatic extension and seminal vesicle invasion primarily reflect local anatomical progression rather than pathological grade itself [12]. Studies of discordance between PI-RADS 5 lesions and targeted biopsy findings have shown that MRI interpretation, lesion localization, and biopsy sampling may all contribute to discrepancies between MRI and pathological findings [13]. Thus, although PI-RADS and conventional MRI features are clinically important, they do not fully capture the risk of higher pathological grade.

PSAD is calculated as the ratio of serum tPSA to prostate volume and incorporates prostate size into the interpretation of PSA, thereby providing a gland-size-adjusted risk measure [14]. In the present study, Model 2 significantly outperformed Model 1 in terms of model fit, indicating that conventional MRI features provided incremental information. The subsequent addition of PSAD further improved model fit and discrimination, and PSAD had the largest partial likelihood ratio χ^2 among the included predictors. This finding does not imply that PI-RADS or conventional MRI features lack value; rather, it suggests that PSAD and MRI information may partly overlap while also providing complementary information. Notably, among the 48 patients with PI-RADS ≤3, 29 (60.4%) had ISUP grade group ≥3. Median PSAD was numerically higher in the MRI-underestimated phenotype than in the concordant-low phenotype, and within the PI-RADS ≤3 subgroup, each doubling of PSAD remained significantly associated with ISUP grade group ≥3. Previous multicenter studies have likewise shown that the risk of clinically significant prostate cancer among patients with PI-RADS 3 lesions increases with higher PSAD. Other studies have also reported that combining PSAD with PI-RADS improves risk assessment for clinically significant prostate cancer across specific PSA ranges and PI-RADS categories [15-17]. These findings suggest that PSAD may provide useful complementary information for patients with relatively low PI-RADS scores who nevertheless require further assessment of pathological risk.

Patient-level bootstrap resampling was used for internal validation, thereby avoiding the loss of information that would have resulted from randomly splitting a sample of 171 patients into separate training and validation sets. Previous methodological studies have shown that, in limited samples, model performance estimates obtained from a single random split may be highly uncertain, whereas resampling methods such as bootstrap validation or repeated cross-validation are generally more appropriate than reliance on a single data partition [18, 19]. Evaluation of prediction models should also consider discrimination, calibration, and

overall prediction error rather than relying solely on the apparent AUROC [20]. In this study, Model 3 showed good out-of-bag discrimination for ISUP grade group ≥2, ≥3, and ≥4, with calibration slopes generally close to 1. By contrast, performance was weaker for grade group 5, for which the AUROC was lower and the calibration slope was 0.75. A calibration slope below 1 generally indicates overly extreme predicted probabilities, which may reflect model overfitting or sampling instability. The predicted probabilities for the highest ISUP grade group should therefore be interpreted cautiously [21].

After patients with tPSA >100 ng/mL were excluded, the OR for each doubling of PSAD was 2.36, which was similar in direction and magnitude to the primary estimate. The PSAD effect also remained stable when PI-RADS was modeled as a continuous variable, MRI lesion extent was coded differently, the analysis was restricted to patients undergoing transrectal biopsy, or additional adjustment was made for biopsy approach, total number of biopsy cores, or BMI. These findings argue against the primary conclusion being driven by a particular method of handling high tPSA values, variable coding, or biopsy approach. Nevertheless, sensitivity analyses demonstrate consistency across alternative analytical settings only; they cannot eliminate potential bias inherent in a retrospective study or substitute for independent external validation.

This study has several limitations. First, it was a single-center retrospective study that included only patients with complete data who were diagnosed with prostate cancer at initial systematic biopsy; patients with negative biopsy findings were not included. Accordingly, the results reflect the conditional distribution of the highest ISUP grade group conditional on biopsy-confirmed prostate cancer and should not be extrapolated to the general population being considered for prostate biopsy. Second, tPSA was recorded only as ">100 ng/mL" in 53 patients, and a value of 100 ng/mL was used to calculate PSAD. This approach may have compressed differences among patients with very high tPSA levels. Although the sensitivity analysis produced consistent findings, the influence of this data limitation cannot be completely excluded. Third, the highest ISUP grade group was determined from systematic biopsy specimens and may have been affected by tumor heterogeneity and sampling error; it therefore cannot fully substitute for the final pathological grade obtained from radical prostatectomy specimens. Fourth, the sample size was limited, the distribution across ISUP grade groups was imbalanced, and only internal validation was performed. The stability and generalizability of the findings therefore require confirmation in independent cohorts with appropriate sample-size planning.

In conclusion, among patients with prostate cancer diagnosed at initial systematic prostate biopsy, PSAD was independently associated with the highest biopsy ISUP grade group and provided incremental risk information beyond the PI-RADS score and conventional MRI features. PSAD may be particularly useful for identifying patients with relatively low PI-RADS scores but higher biopsy ISUP grade groups. Future studies should externally validate these findings in larger, more diverse independent cohorts with broader disease spectra and further assess whether incorporating PSAD provides meaningful benefits for clinical decision-making and patient outcomes.

Acknowledgements

This study was supported by the Basic Research Special Project (General Program) of the Yunnan Provincial Department of Science and Technology (grant no. 202401AT070073).

Disclosure of conflict of interest

None.

Address correspondence to: Chunmei Zhang, Department of Pathology, The First Affiliated Hospital of Dali University, No. 32 Jiasibo Road, Dali 671000, Yunnan, China. E-mail: zhangchunmeiemail@163.com

References

[1] Cornford P, van den Bergh RCN, Briers E, Van den Broeck T, Brunckhorst O, Darraugh J, Eberli D, De Meerleer G, De Santis M, Farolfi A, Gandaglia G, Gillessen S, Grivas N, Henry AM, Lardas M, van Leenders GJLH, Liew M, Linares Espinos E, Oldenburg J, van Oort IM, Oprea-Lager DE, Ploussard G, Roberts MJ, Rouvière O, Schoots IG, Schouten N, Smith EJ, Stranne

J, Wiegel T, Willemse PM and Tilki D. EAU-EANM-ESTRO-ESUR-ISUP-SIOG guidelines on prostate cancer-2024 update. Part I: screening, diagnosis, and local treatment with curative intent. Eur Urol 2024; 86: 148-163.
[2] Agosti V and Munari E. Histopathological evaluation and grading for prostate cancer: current issues and crucial aspects. Asian J Androl 2024; 26: 575-581.
[3] Oerther B, Nedelcu A, Engel H, Schmucker C, Schwarzer G, Brugger T, Schoots IG, Eisenblaetter M, Sigle A, Gratzke C, Bamberg F and Benndorf M. Update on PI-RADS version 2.1 diagnostic performance benchmarks for prostate MRI: systematic review and meta-analysis. Radiology 2024; 312: e233337.
[4] Lin Y, Johnson LA, Fennessy FM and Turkbey B. Prostate cancer local staging with magnetic resonance imaging. Radiol Clin North Am 2024; 62: 93-108.
[5] Stanzione A, Lee KL, Sanmugalingam N, Rajendran I, Sushentsev N, Caglič I and Barrett T. Expect the unexpected: investigating discordant prostate MRI and biopsy results. Eur Radiol 2024; 34: 4810-4820.
[6] Wang S, Kozarek J, Russell R, Drescher M, Khan A, Kundra V, Barry KH, Naslund M and Siddiqui MM. Diagnostic performance of prostate-specific antigen density for detecting clinically significant prostate cancer in the era of magnetic resonance imaging: a systematic review and meta-analysis. Eur Urol Oncol 2024; 7: 189-203.
[7] Frisbie JW, Van Besien AJ, Lee A, Xu L, Wang S, Choksi A, Afzal MA, Naslund MJ, Lane B, Wong J, Wnorowski A and Siddiqui MM. PSA density is complementary to prostate MP-MRI PI-RADS scoring system for risk stratification of clinically significant prostate cancer. Prostate Cancer Prostatic Dis 2023; 26: 347-352.
[8] Nguyen TA, Fourcade A, Zambon A, Saout K, Deruelle C, Joulin V, Tissot V, Doucet L, Rozet F, Fournier G and Valeri A. Optimal PSA density threshold and predictive factors for the detection of clinically significant prostate cancer in patient with a PI-RADS 3 lesion on MRI. Urol Oncol 2023; 41: 354.e11-354.e18.
[9] Pellegrino F, Stabile A, Sorce G, Quarta L, Robesti D, Cannoletta D, Cirulli G, Barletta F, Scuderi S, Mazzone E, de Angelis M, Brembilla G, De Cobelli F, Salonia A, Montorsi F, Briganti A and Gandaglia G. Added value of prostate-specific antigen density in selecting prostate biopsy candidates among men with elevated prostate-specific antigen and PI-RADS ≥3 lesions on multiparametric magnetic resonance imaging of the prostate: a systematic assessment by PI-RADS score. Eur Urol Focus 2024; 10: 634-640.
[10] Yilmaz EC, Shih JH, Belue MJ, Harmon SA, Phelps TE, Garcia C, Hazen LA, Toubaji A, Merino MJ, Gurram S, Choyke PL, Wood BJ, Pinto PA and Turkbey B. Prospective evaluation of PI-RADS version 2.1 for prostate cancer detection and investigation of multiparametric mri-derived markers. Radiology 2023; 307: e221309.
[11] Ayranci A, Caglar U, Meric A, Gelmis M, Sarilar O and Ozgor F. Effects of the lesion size on clinically significant prostate cancer detection rates in PI-RADS category 3-5 lesions. Actas Urol Esp (Engl Ed) 2024; 48: 526-531.
[12] Oliveira T, Amaral Ferreira L, Marto CM, Marques C, Oliveira C and Donato P. The role of multiparametric MRI in the local staging of prostate cancer. Front Biosci (Elite Ed) 2023; 15: 21.
[13] Arcot R, Sekar S, Kotamarti S, Krischak M, Michael ZD, Foo WC, Huang J, Polascik TJ and Gupta RT. Structured approach to resolving discordance between PI-RADS v2.1 score and targeted prostate biopsy results: an opportunity for quality improvement. Abdom Radiol (NY) 2022; 47: 2917-2927.
[14] Robinson E, Kinsella N, Ap Dafydd D, Shur J, Sohaib A, Hazell S, Bassett P, Kumar P, Mayer E, Cahill D and Withey SJ. Prostate specific antigen density and clinically-significant prostate cancer: the influence of prostatic volume. Prostate 2025; 85: 784-791.
[15] Drevik J, Dalimov Z, Uzzo R, Danella J, Guzzo T, Belkoff L, Raman J, Tomaszewski J, Trabulsi E, Reese A, Singer EA, Syed K, Jacobs B, Correa A, Smaldone M and Ginzburg S. Utility of PSA density in patients with PI-RADS 3 lesions across a large multi-institutional collaborative. Urol Oncol 2022; 40: 490.e1-490.e6.
[16] Wen J, Liu W, Shen X and Hu W. PI-RADS v2.1 and PSAD for the prediction of clinically significant prostate cancer among patients with PSA levels of 4-10 ng/ml. Sci Rep 2024; 14: 6570.
[17] Wei X, Xu J, Zhong S, Zou J, Cheng Z, Ding Z and Zhou X. Diagnostic value of combining PI-RADS v2.1 with PSAD in clinically significant prostate cancer. Abdom Radiol (NY) 2022; 47: 3574-3582.
[18] Eertink JJ, Heymans MW, Zwezerijnen GJC, Zijlstra JM, de Vet HCW and Boellaard R. External validation: a simulation study to compare cross-validation versus holdout or external testing to assess the performance of clinical prediction models using PET data from DLBCL patients. EJNMMI Res 2022; 12: 58.
[19] Steyerberg EW. Validation in prediction research: the waste by data splitting. J Clin Epidemiol 2018; 103: 131-133.

[20] Collins GS, Dhiman P, Ma J, Schlussel MM, Archer L, Van Calster B, Harrell FE Jr, Martin GP, Moons KGM, van Smeden M, Sperrin M, Bullock GS and Riley RD. Evaluation of clinical prediction models (part 1): from development to external validation. BMJ 2024; 384: e074819.

[21] Van Calster B, McLernon DJ, van Smeden M, Wynants L and Steyerberg EW; Topic Group "Evaluating diagnostic tests and prediction models" of the STRATOS initiative. Calibration: the Achilles heel of predictive analytics. BMC Med 2019; 17: 230.